Available online at http://scik.org
Commun. Math. Biol. Neurosci. 2023, 2023:129
https://doi.org/10.28919/cmbn/8265
ISSN: 2052-2541

EVALUATING RECURRENT NEURAL NETWORKS AND LONG SHORT-TERM MEMORY FOR AIR POLLUTION FORECASTING: MITIGATING THE IMPACT OF VOLATILE ENVIRONMENTAL FACTORS

FATKHUROKHMAN FAUZI[1,4,*], ROCHDI WASONO[1,3], IQBAL KHARISUDIN[2]

[1]Department of Statistics, Universitas Muhammadiyah Semarang, Semarang 50273, Indonesia

[2]Statistics and Data Science Study Program, Universitas Negeri Semarang, Semarang 50229, Indonesia

[3]Health and Environmental Research Laboratory, Universitas Muhammadiyah Semarang, Semarang 50273, Indonesia

[4]Computing and Data Science Research Laboratory, Universitas Muhammadiyah Semarang, Semarang 50273, Indonesia

Abstract: Mitigation is the key to reducing the negative effects caused by air pollution. Forecasting several periods into the future is needed to understand the picture of air pollution as a basis for mitigation. Choosing the right forecasting method is crucial. This research will evaluate two machine learning methods, namely Recurrent Neural Network (RNN) and Long Short-Term Memory (LSTM) for air pollution forecasting. Air pollution data for the Jakarta area is the object of research. The data is divided into two parts, namely 80% training data and 20% testing data. Both methods were evaluated with Mean Square Error (MSE), Mean Absolute Error (MAE), and Root Mean Square Error (RMSE). The best method is the method that has the smallest MSE, MAE, and RMSE values. We experimented with a combination of hidden layer and epoch values. The results obtained are that air pollution in the Jakarta area is very volatile and is influenced by the COVID-19 pandemic. The correlation between NO2 and CO particles is the highest compared to other particles. The RNN method works well on PM10, O3, and NO2 particles. Meanwhile, the LSTM

---

*Corresponding author
E-mail address: fatkhurokhmanf@unimus.ac.id
Received October 08, 2023

method works well on SO2 and CO particles. The best hidden layer and epoch values are 50 and 150 and 100 and 200.

Keywords: air pollution; recurrent neural network; long short-term memory; comparison.

2020 AMS Subject Classification: 68T07.

1. INTRODUCTION

Air pollution is one of the greatest environmental threats to human health and organisms throughout the world [1]. Poor air quality can contribute to more than 6 million deaths a year worldwide. The economic losses from air pollution are very large, estimated at US$ 8T or equivalent to IDR 123,000 T [1]. Air pollution can be caused by two sources, namely moving and non-moving, including the industrial sector, power plants, vehicle emissions, and domestic. The Special Region of Jakarta (DKI) is one of the cities in Indonesia, which is ranked 1st as a country that has the highest level of air pollution in Southeast Asia, with an annual average $PM_{2.5}$ concentration of 36.2 μg/m^3 [1].

The particles that are a reference for the high and low levels of air pollution in Indonesia are Particulates with a diameter of 10 micrometres (μm) (PM_{10}), Sulphur Dioxide (SO_2), Ozone (O_3), Nitrogen dioxide (NO_2), and Carbon Monoxide (CO). These particles can come from motorized vehicles, industry and human activities [2]. The effects of air pollution in Jakarta are that more than 7,000 children experience respiratory problems, 10,000 deaths, and 500 hospitalizations [3]. SO_X, NO_X, CO_2, CH_4, NH_3, TSP, PB, PM_{10}, $PM_{2.5}$ and Nitrogen are pollutants that contribute 93.70% of environmental damage due to air pollution [4].

Air pollution mitigation needs to be done to prevent the worst possibility. Forecasting air pollution in the future is one solution. The accuracy of the forecasting method is very crucial, and the choice of method is very important. Methods with high accuracy can produce appropriate mitigation decisions. Several studies have applied forecasting to mitigate air pollution disasters [5–7].

Various methods have been proposed, including Autoregressive Moving Average (ARIMA), Exponential Smoothing, and Vector Autoregressive [8–10]. The ARIMA method can only be used on linear data patterns, while pollution data patterns are mostly non-linear [11,12]. The effect is poor accuracy in predictions.

Neural network-based methods are very reliable on data with non-linear patterns. These non-linear methods include Recurrent Neural Networks (RNN) and Long Short-Term Memory (LSTM) [13]. Alhirmizy et al. [14] applied the LSTM method to predict air pollution in the Spanish city of Madrid. This research concludes that the LSTM method works very well in predicting air pollution in the city of Madrid. Experiments comparing the RNN LSTM and ARIMA methods by Tokgöz et al. [15] resulted in non-linear methods having superior performance compared to ARIMA. Several studies have applied RNN and LSTM methods for forecasting [16–20].

Determining the method in forecasting cases is very crucial; a good method will produce the right mitigation decisions. This research will investigate the ability of the RNN and LSTM methods to predict air pollution in Jakarta. We use four parameter scenarios in the RNN and LSTM methods. Determining the best method and scenario is based on the Mean Square Error (MSE), Mean Absolute Error (MAE), and Root Mean Square Error (RMSE) values.

2. RESEARCH METHODOLOGY

The first step is collecting the data from the website (https://data.jakarta.go.id/). The particles measured by the air quality monitoring station in the Special Capital Region (DKI) of Jakarta are Particulates with a diameter of 10 micrometres (μm) (PM_{10}), Sulphur Dioxide (SO_2), Ozone (O_3), Nitrogen dioxide (NO_2), and Carbon Monoxide (CO). Air quality in DKI Jakarta is measured from these five particles. The frequency of data taken is daily, from January 2020 to December 2021.

Before comparing the performance of the Recurrent Neural Network (RNN) and Long Short-Term Memory (LSTM) methods, fill in the missing data by interpolation. The interpolation method approach used is average [21]. We average the values across the same day, month and year to fill in missing data; this is done for all particles. This method is used for characteristics when approached by similar days and months.

A. Recurrent Neural Networks (RNN)

The second step is processing the data using the Recurrent Neural Networks (RNN) method. A Recurrent Neural Network (RNN) is a type of neural network specifically designed to process data sequences with time step indices t ranging from 1 to n. RNNs can also be thought of as having a "memory" that stores details regarding calculations that have already been made [22].

Given an input sequence of length $x = (x_1, x_2, \ldots, x_T)$, a general equation for the RNN hidden state is as follows[23]:

$$\boldsymbol{h}_t = \begin{cases} 0, if\ (t = 0) \\ \phi(h_{t-1}, x_t), otherwise \end{cases} \tag{1}$$

Non-linear function represented by ϕ. The recurrent hidden state's ($\boldsymbol{h}_t$) updating is accomplished as:

$$\boldsymbol{h}_t = g(\boldsymbol{W}x_t + \boldsymbol{U}\boldsymbol{h}_{t-1} + \boldsymbol{b}) \quad (2)$$

Hyperbolic tangent function represented by g. $\boldsymbol{W}$ dan $\boldsymbol{U}$ describe the weight matrix that can be adjusted to the hidden state and data values, and b is the bias.

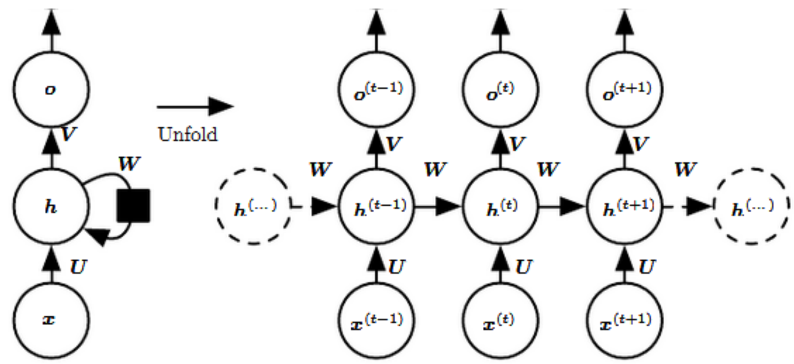

Figure 1. Basic of RNN [24]

B. Long Short-Term Memory (LSTM)

Long Short-Term Memory (LSTM) is another form of RNN that can perform learning on long-term dependencies [25,26]. This model was introduced by Hochreiter and Schmidhuber in 1997. All recurrent neural networks have the form of a series of recurrent neural network modules. LSTM also has the same structure but additional features in the form of cell gates.

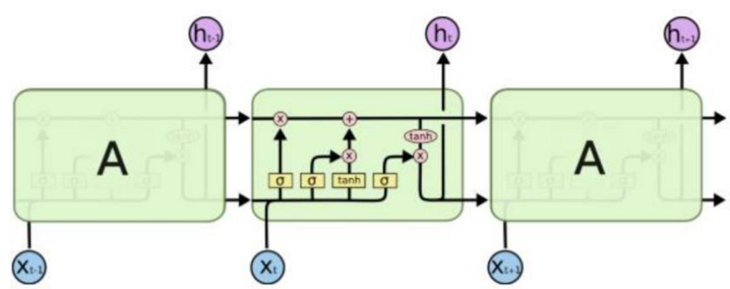

Figure 2. LSTM Structure [27]

The LSTM will determine what information to remove from the cell. The forget gate $\boldsymbol{f}_t$ layer makes this decision. This layer will focus on $\boldsymbol{h}_{t-1}$ and x_t to produce an output between 0 and 1. Output 0 represents that the information will be forgotten, while output 1 represents that the information will not be forgotten.

$$\boldsymbol{f_t} = \sigma(\boldsymbol{W}_f x_t + \boldsymbol{U}_f \boldsymbol{h}_{t-1} + \boldsymbol{b}_f) \tag{3}$$

The logistic sigmoid function is played by $\sigma(.)$, while $\boldsymbol{W}_f$, $\boldsymbol{U}_f$, and $\boldsymbol{b}_f$ are matrix and vector parameters in the forget gate layer.

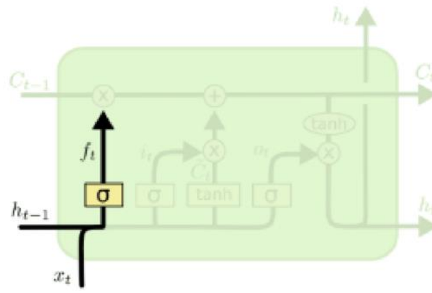

Figure 3. Forget Layer [27]

The next step is determining whether the information will be stored in the cell. First, a sigmoid layer called the "input gate layer" determines which values will be updated. Next, a $tanh$ layer creates a vector of new candidate values, $\tilde{\boldsymbol{c}}_t$, that can be added to the state. These two layers will be combined in the next step to update the state.

$$\tilde{\boldsymbol{c}}_t \ = \ tanh\ (\boldsymbol{W}_{\tilde{c}} x_t + \boldsymbol{U}_{\tilde{c}} \boldsymbol{h}_{t-1} + \boldsymbol{b}_{\tilde{c}}) \tag{4}$$

The $\boldsymbol{c}_t$ value ranges from -1 to 1. Hyperbolic tangent is represented by $tanh(.)$. Meanwhile, the values of $\boldsymbol{W}_{\tilde{c}}$, $\boldsymbol{U}_{\tilde{c}}$, and $\boldsymbol{b}_{\tilde{c}}$ are new parameter matrices and vectors.

$$i_t = \sigma(\boldsymbol{W}_i x_t + \boldsymbol{U}_i \boldsymbol{h}_{t-1} + \boldsymbol{b}_i) \tag{5}$$

Where i_t has a value of 0 to 1, $\boldsymbol{W}_i$, $\boldsymbol{U}_i$, and $\boldsymbol{b}_i$ are parameters obtained from the gate input.

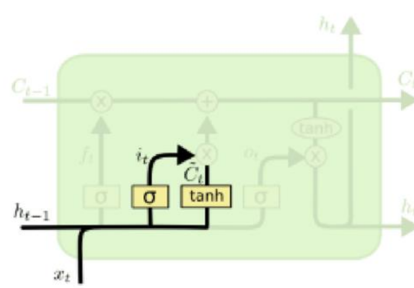

Figure 4. Remember Gate Structure [27]

Next, the old state will be updated, $\boldsymbol{c}_{t-1}$ to the new cell state $\boldsymbol{c}_t$. Then, $\boldsymbol{f}_t$ will be multiplied by the old state by ignoring previously forgotten information. Then, it is added with $\boldsymbol{c}_t$.

$$\boldsymbol{c}_t = \boldsymbol{f}_t \odot \boldsymbol{c}_{t-1} + \boldsymbol{i}_t \odot \widetilde{\boldsymbol{c}}_t \quad (6)$$

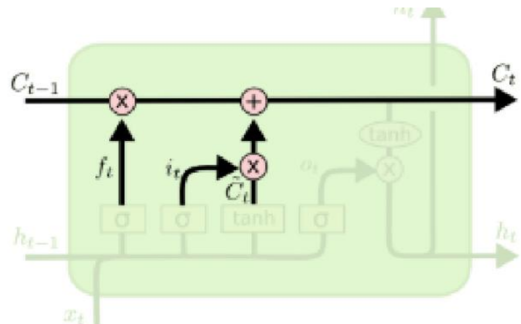

Figure 5. Update Layer Structure [27]

The final step is to determine what the output is. First, the sigmoid layer will determine the part of the cell that will be removed. Then, the cell will be passed to the $tanh$ layer (to force the output value between -1 and 1) and multiplied by the output of the sigmoid gate.

$$\boldsymbol{o}_t = \sigma(\boldsymbol{W}_o x_t + \boldsymbol{U}_o \boldsymbol{h}_{t-1} + \boldsymbol{b}_o) \quad (7)$$

Where $\boldsymbol{W}_o$, $\boldsymbol{U}_o$, and $\boldsymbol{b}_o$ are parameters in the form of a matrix and vector from the gate output. $\boldsymbol{o}_t$ is a vector with values 0 to 1.

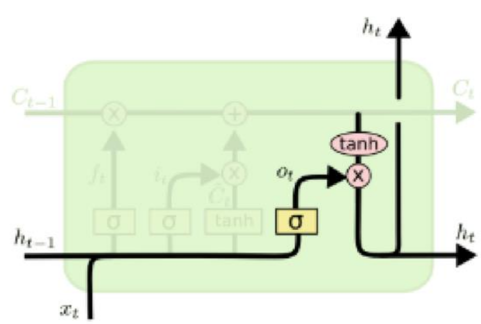

Figure 6. Output Layer Structure [27]

$$\boldsymbol{h}_t = \tanh\,(c_t) \odot \boldsymbol{o}_t \quad (9)$$

The combination of equations 6 and 7 produces a new hidden state ($\boldsymbol{h}_t$).

C. Accuracy measure

After modelling, the next step is to compare the performance of the RNN and LSTM methods. We chose three measures of model goodness, namely Mean Square Error (MSE) , Mean Absolute Error (MAE), and Root Mean Square Error (RMSE) [28–30].. The formula for the three sizes is as follows:

$$MSE = \frac{1}{n}\sum_{i=1}^{n}\left(\widehat{\boldsymbol{Y}}_i - \boldsymbol{Y}_i\right)^2 \tag{10}$$

$$MAE = \frac{1}{n}\sum_{i=1}^{n}\left|\widehat{\boldsymbol{Y}}_i - \boldsymbol{Y}_i\right| \tag{11}$$

$$RMSE = \sqrt{\frac{1}{n}\sum_{i=1}^{n}\left(\widehat{\boldsymbol{Y}}_i - \boldsymbol{Y}_i\right)^2} \tag{12}$$

$\boldsymbol{Y}_i$ is a vector of actual values, $\widehat{\boldsymbol{Y}}_i$ is a vector of predicted values, and n is the amount of data. The method with the smallest MSE, MAE, and RMSE values is best.

3. RESULT AND DISCUSSION

A. Characteristics of Pollution in Jakarta

In this research, the characteristics of air pollution in Jakarta need to be known before comparing the ability of the RNN and LSTM methods to predict air pollution. Characteristics can be identified through measures of central tendency and data graphs. The results of the characteristic analysis are method recommendations.

Figure 7 shows that the air quality in DKI Jakarta generally fluctuates, especially in 2020. The COVID-19 phenomenon occurred in early 2020, but the effect on community activities in Indonesia occurred at the end of 2020. The policy of limiting activities is a form of preventing COVID-19. COVID-19 has a positive impact on air pollution in DIKI Jakarta. Air pollution in 2021 will decrease significantly, especially O3, SO2 and NO_2. The COVID-19 pandemic hurts humans but positively impacts the environment, especially air pollution [31]. Fu et al. [32] found a significant decrease during the lockdown period, especially NO_2 particles.

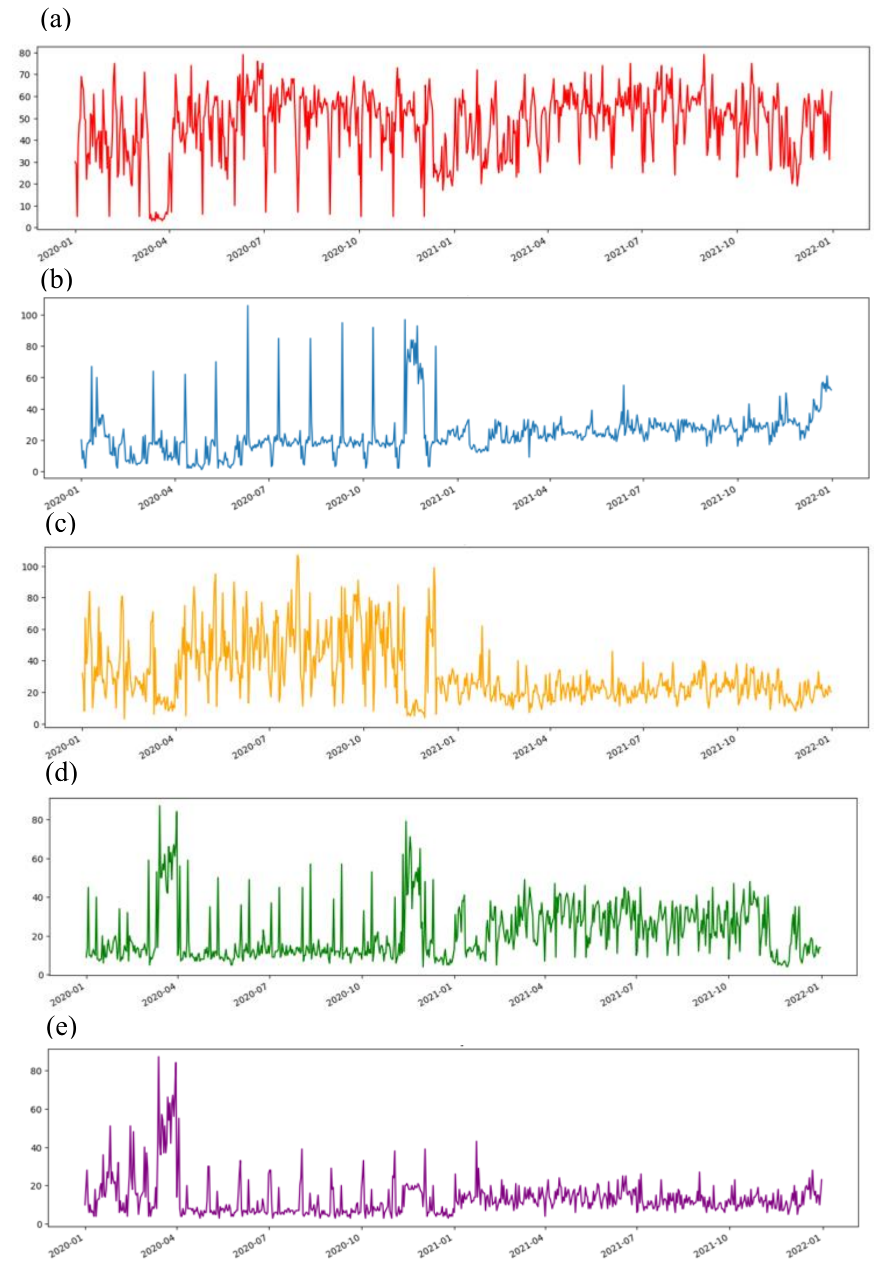

Figure 7. Time Series for Pollutant in DKI Jakarta

(a) PM_{10}, (b) SO_2, (c) O_3, (d) NO_2, and (e) CO

The maximum values for PM_{10} and SO_2 particles were highest in September 2020, while the lowest occurred in March and April 2020. The relationship between PM_{10} and SO_2 particles was significant at 0.2. For O_3 and NO_2 particles, the lowest was in September 2020; the correlation between the two was significantly negative at 0.45. The COVID-19 pandemic has significantly impacted CO particles; a drastic decrease in March shows this.

Table 1. Descriptive Statistics

No	Variable (Particle)	Mean	Minimum	Maximum	Standard Deviation
	PM_{10}	47.34	3.00	79.00	15.48
	SO_2	23.68	1.00	106.00	14.24
	CO	13.33	3.00	87.00	10.05
	O_3	31.80	3.00	107.00	19.60
	NO_2	21.40	4.00	87.00	14.00

B. Correlation Between Particle

The relationship between particles can be seen in Figure 8. The highest correlation is between CO and NO_2 particles at 0.62. These two particles simultaneously come out of the combustion of motor vehicles. Meanwhile, the correlation between O_3 and NO_2 is significantly negative, caused by different data fluctuations between the two particles. Particles that have an insignificant relationship are PM_{10} and NO_2 as well as SO_2 and CO.

Figure 8. Matrix Correlation

We enter the core of this research, namely the performance comparison between the RNN and LSTM methods. Analysis of the performance of the RNN and LSTM methods was carried out univariately on each air pollution particle. We determined the hidden layers to be 50 and 150, while the Epoch values used were 100 and 200. The evaluation was carried out by looking at the most miniature Mean Square Error (MSE), Mean Absolute Error (MAE), and Root Mean Square Error (RMSE) values.

C. Comparison of RNN and LSTM Performance

We start the comparison by setting the Hidden Layer values at 50 and 150 while the epoch values are 100 and 200. The Hidden Layer and epoch values will be combined to obtain good accuracy for the RNN and LSTM methods. We use Adam optimization to get the best parameters.

Table 2. RNN vs LSTM Performance Comparison

No	Particle	Methods	Hidden Layer	Epoch	MSE	MAE	RMSE
1	PM_{10}	RNN	50	100	0.015399	0.094899	0.124095
			50	200	0.015759	0.096241	0.125536
			150	100	0.015476	0.098598	0.124404
			150	200	0.015632	0.097281	0.125029
		LSTM	50	100	0.018927	0.111265	0.137575
			50	200	0.017463	0.104785	0.132148
			150	100	0.017988	0.107047	0.134118
			150	200	0.017262	0.104443	0.131385
2	SO_2	RNN	50	100	0.003145	0.036910	0.056079
			50	200	0.003103	0.035965	0.055703
			150	100	0.003193	0.035882	0.056503
			150	200	0.003227	0.036765	0.056804
		LSTM	50	100	0.003569	0.037355	0.059738
			50	200	0.003091	0.034827	0.055598
			150	100	0.003019	0.034445	0.054949
			150	200	0.003186	0.035381	0.056441
3	NO_2	RNN	50	100	0.007742	0.060401	0.087991
			50	200	0.007723	0.059858	0.087880
			150	100	0.007853	0.060330	0.088615
			150	200	0.007611	0.059039	0.087243
		LSTM	50	100	0.009305	0.069454	0.096464
			50	200	0.008131	0.066655	0.090171
			150	100	0.008540	0.066764	0.092412
			150	200	0.007830	0.062725	0.088490

No	Particle	Methods	Hidden Layer	Epoch	MSE	MAE	RMSE
4	O_3	RNN	50	100	0.002490	0.039568	0.049900
			50	200	0.002643	0.041272	0.051407
			150	100	0.002569	0.040457	0.050690
			150	200	0.002350	0.037817	0.048480
		LSTM	50	100	0.002993	0.044957	0.054710
			50	200	0.002851	0.043534	0.053398
			150	100	0.002943	0.044288	0.054246
			150	200	0.002591	0.041245	0.050899
5	CO	RNN	50	100	0.002046	0.034828	0.045230
			50	200	0.002092	0.035464	0.045734
			150	100	0.002086	0.036342	0.045678
			150	200	0.002193	0.038081	0.046829
		LSTM	50	100	0.002168	0.037474	0.046565
			50	200	0.001955	0.034319	0.044211
			150	100	0.001978	0.035577	0.044470
			150	200	0.001886	0.034077	0.043430

Based on Table 2, the RNN method generally performs better than the LSTM method, except for CO and SO_2 particles. Hidden Layer 50 and Epoch 100 are the best parameters for PM_{10} and O_3 particles. For particle NO_2, the best RNN parameters are hidden layer 150 and epoch 200. For LSTM parameters for particles CO and SO_2, the best hidden layer is 150, while the best epoch is 100 and 200.

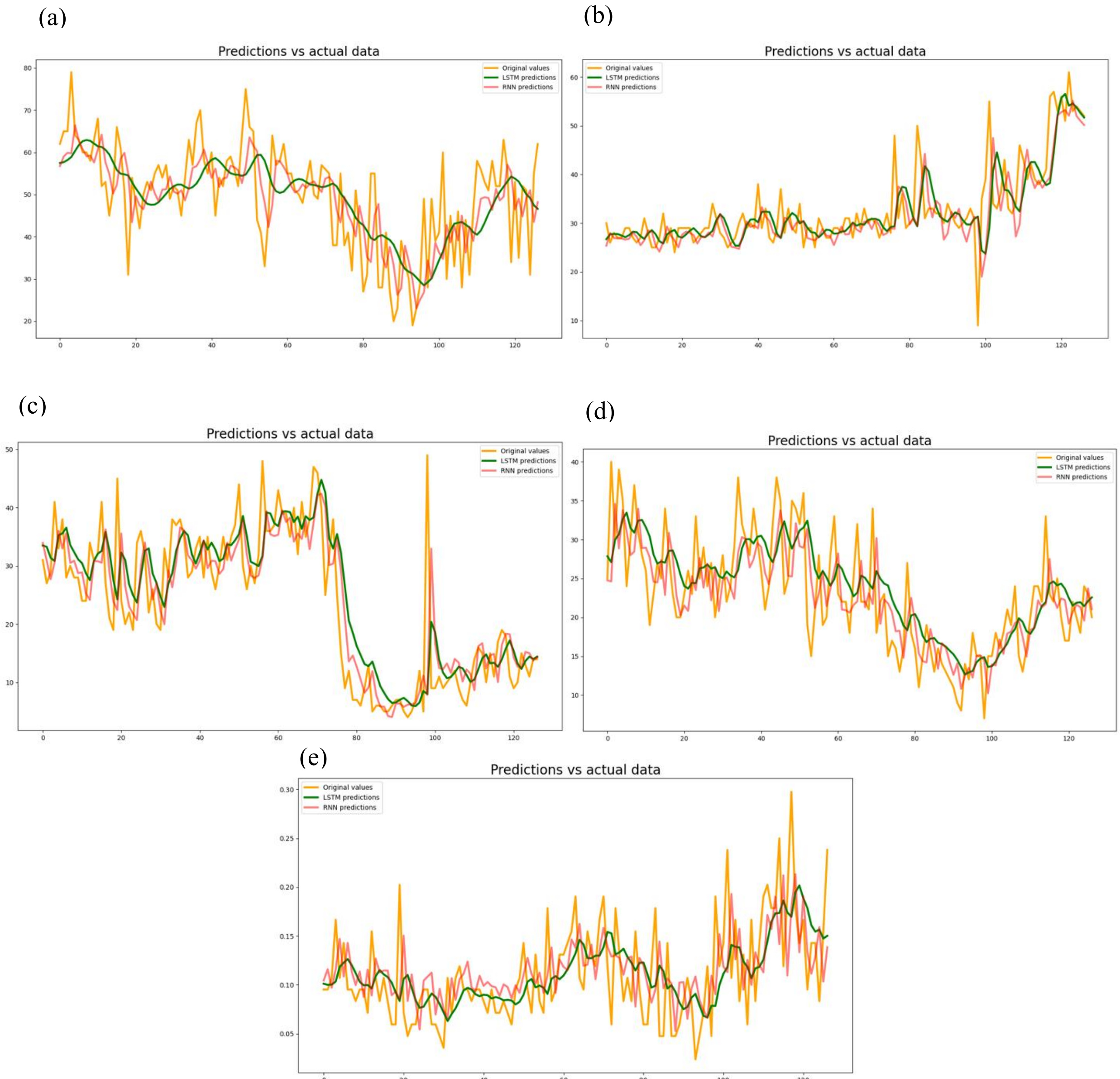

Figure 9. Comparing Between Original dataset and RNN, LSTM Prediction (a) PM_{10} (b) SO_2 (c) NO_2 (d) O_3 (e) CO

The RNN method followed the original data pattern better than the LSTM method for PM_{10}, NO_2, and O_3 particles. For PM_{10} particles, the LSTM method cannot follow the data pattern well. Meanwhile, for NO_2 and O_3 particles, the LSTM method follows the original data pattern quite well, but it does not work in extreme situations. The results in Figure 9 are in line with the results in Table 2.

4. Conclusion

Pollution in Jakarta fluctuated at the beginning of 2020, decreasing significantly at the end 2020 due to the lockdown. However, PM_{10} particles have different conditions, with extreme fluctuations throughout 2020-2021. NO_2 and CO have the strongest correlation between particles. The RNN method works better than the LSTM method on three particles (PM_{10}, O_3, and NO_2), while the LSTM method works well on SO_2 and CO particles. The best hidden layers are 50 and 150, while the best epochs are 100 and 200. For further research, hybrid methods need to be applied to improve performance.

Acknowledgement

Acknowledgements to research institutes and community service, Universitas Muhammadiyah Semarang for funding this research with contract number 048/UNIMUS.L/PG/PJ.INT/2023.

Conflict of Interests

The authors declare that there was no conflict of interest in the writing process.

References

[1] IQAir, 2022 World air quality report, 2022. https://www.iqair.com/newsroom/world-air-quality-report-press-release-2022.

[2] S. Kashima, T. Yorifuji, T. Tsuda, et al. Effects of traffic-related outdoor air pollution on respiratory illness and mortality in children, taking into account indoor air pollution, in Indonesia, J. Occup. Environ. Med, 52 (2010), 340-345.

[3] G. Syuhada, A. Akbar, D. Hardiawan, et al. Impacts of air pollution on health and cost of illness in Jakarta, Indonesia, Int. J. Environ. Res. Public Health. 20 (2023), 2916. https://doi.org/10.3390/ijerph20042916.

[4] V. Pirmana, A.S. Alisjahbana, A.A. Yusuf, et al. Environmental costs assessment for improved environmental-economic account for Indonesia, J. Clean. Product. 280 (2021), 124521. https://doi.org/10.1016/j.jclepro.2020.124521.

[5] S.M.S. Cabaneros, J.K.S. Calautit, B.R. Hughes, Hybrid artificial neural network models for effective prediction and mitigation of urban roadside NO2 pollution, Energy Procedia. 142 (2017), 3524-3530. https://doi.org/10.1016/j.egypro.2017.12.240.

[6] W. Zhou, X. Wu, S. Ding, et al. Predictions and mitigation strategies of PM2.5 concentration in the Yangtze

River Delta of China based on a novel nonlinear seasonal grey model, Environ. Pollution. 276 (2021), 116614. https://doi.org/10.1016/j.envpol.2021.116614.

[7] A.H. Bukhari, M.A.Z. Raja, M. Shoaib, et al. Fractional order Lorenz based physics informed SARFIMA-NARX model to monitor and mitigate megacities air pollution, Chaos Solitons Fractals. 161 (2022), 112375. https://doi.org/10.1016/j.chaos.2022.112375.

[8] A.D. Syafei, N. Ramadhan, J. Hermana, et al. Application of exponential smoothing holt winter and ARIMA models for predicting air pollutant concentrations, EnvironmentAsia. 11 (2018), 251-262. https://doi.org/10.14456/EA.2018.52.

[9] P. Gopu, R.R. Panda, N.K. Nagwani, Time series analysis using ARIMA model for air pollution prediction in Hyderabad City of India, in: V.S. Reddy, V.K. Prasad, J. Wang, K.T.V. Reddy (Eds.), Soft Computing and Signal Processing, Springer Singapore, Singapore, 2021: pp. 47–56. https://doi.org/10.1007/978-981-33-6912-2_5.

[10] X. Li, F. Huang, Empirical study on the relationship between agricultural economic structure growth and environmental pollution based on time-varying parameter vector autoregressive model, J. Environ. Public Health. 2022 (2022), 5684178. https://doi.org/10.1155/2022/5684178.

[11] J. Luo, Y. Gong, Air pollutant prediction based on ARIMA-WOA-LSTM model, Atmos. Pollut. Res. 14 (2023), 101761. https://doi.org/10.1016/j.apr.2023.101761.

[12] X. Li, F. Huang, Empirical study on the relationship between agricultural economic structure growth and environmental pollution based on time-varying parameter vector autoregressive model, J. Environ. Public Health. 2022 (2022), 5684178. https://doi.org/10.1155/2022/5684178.

[13] I. Kharisudin, F. Fauzi, M. Iqbal, et al. Electricity load forecasting using long short-term memory: Case study from Central Java and DIY, AIP Conf. Proc. 2614 (2023), 040062.

[14] S. Alhirmizy, B. Qader, Multivariate time series forecasting with LSTM for Madrid, Spain pollution, in: 2019 International Conference on Computing and Information Science and Technology and Their Applications (ICCISTA), IEEE, Kirkuk, Iraq, 2019: pp. 1–5. https://doi.org/10.1109/ICCISTA.2019.8830667.

[15] A. Tokgoz, G. Unal, A RNN based time series approach for forecasting turkish electricity load, in: 2018 26th Signal Processing and Communications Applications Conference (SIU), IEEE, Izmir, 2018: pp. 1–4. https://doi.org/10.1109/SIU.2018.8404313.

[16] S. Singh, V. Kumar, Z. Ahmed, et al. Delhi air pollution prediction: a comparative analysis using time series forecasting, in: 2023 International Conference on Disruptive Technologies (ICDT), IEEE, Greater Noida, India, 2023: pp. 604–608. https://doi.org/10.1109/ICDT57929.2023.10151445.

[17] M. Ansari, M. Alam, An intelligent IoT-cloud-based air pollution forecasting model using univariate time-series analysis, Arab J. Sci Eng. (2023). https://doi.org/10.1007/s13369-023-07876-9.

[18] H. Liao, L. Yuan, M. Wu, et al. Air quality prediction by integrating mechanism model and machine learning model, Sci. Total Environ. 899 (2023), 165646. https://doi.org/10.1016/j.scitotenv.2023.165646.

[19] C. Erden, Genetic algorithm-based hyperparameter optimization of deep learning models for PM2.5 time-series prediction, Int. J. Environ. Sci. Technol. 20 (2023), 2959-2982. https://doi.org/10.1007/s13762-023-04763-6.

[20] I. Kharisudin, F. Fauzi, M. Iqbal, et al. Electricity load forecasting using long short-term memory: Case study from Central Java and DIY, AIP Conf. Proc. 2614 (2023), 040062. https://doi.org/10.1063/5.0126313.

[21] S.J. Hadeed, M.K. O'Rourke, J.L. Burgess, et al. Imputation methods for addressing missing data in short-term monitoring of air pollutants, Sci. Total Environ. 730 (2020), 139140. https://doi.org/10.1016/j.scitotenv.2020.139140.

[22] A.X.M. Chang, E. Culurciello, Hardware accelerators for recurrent neural networks on FPGA, in: 2017 IEEE International Symposium on Circuits and Systems (ISCAS), IEEE, Baltimore, MD, USA, 2017: pp. 1–4. https://doi.org/10.1109/ISCAS.2017.8050816.

[23] P. Bahad, P. Saxena, R. Kamal, Fake news detection using bi-directional LSTM-recurrent neural network, Procedia Computer Sci. 165 (2019), 74-82. https://doi.org/10.1016/j.procs.2020.01.072.

[24] M. Gao, G. Shi, S. Li, Online prediction of ship behavior with automatic identification system sensor data using bidirectional long short-term memory recurrent neural network, Sensors. 18 (2018), 4211. https://doi.org/10.3390/s18124211.

[25] Y. Zhang, R. Xiong, H. He, et al. Long short-term memory recurrent neural network for remaining useful life prediction of lithium-ion batteries, IEEE Trans. Veh. Technol. 67 (2018), 5695-5705. https://doi.org/10.1109/tvt.2018.2805189.

[26] J. Lei, C. Liu, D. Jiang, Fault diagnosis of wind turbine based on Long Short-term memory networks, Renew. Energy. 133 (2019), 422-432. https://doi.org/10.1016/j.renene.2018.10.031.

[27] J. Ju, F.A. Liu, Multivariate time series data prediction based on ATT-LSTM network, Appl. Sci. 11 (2021), 9373. https://doi.org/10.3390/app11209373.

[28] A. Atalan, Forecasting drinking milk price based on economic, social, and environmental factors using machine learning algorithms, Agribusiness. 39 (2022), 214–241. https://doi.org/10.1002/agr.21773.

[29] C. Kiganda, M.A. Akcayol, Forecasting the spread of COVID-19 using deep learning and big data analytics methods, SN Computer Sci. 4 (2023), 374. https://doi.org/10.1007/s42979-023-01801-5.

[30] A. Jierula, S. Wang, T.M. OH, et al. Study on accuracy metrics for evaluating the predictions of damage locations in deep piles using artificial neural networks with acoustic emission data, Appl. Sci. 11 (2021), 2314. https://doi.org/10.3390/app11052314.

[31] S.A.M. Khalifa, M.M. Swilam, A.A.A. El-Wahed, et al. Beyond the pandemic: COVID-19 pandemic changed

the face of life, Int. J. Environ. Res. Public Health. 18 (2021), 5645. https://doi.org/10.3390/ijerph18115645.
[32] F. Fu, K.L. Purvis-Roberts, B. Williams, Impact of the COVID-19 pandemic lockdown on air pollution in 20 major cities around the world, Atmosphere. 11 (2020), 1189. https://doi.org/10.3390/atmos11111189.